



# Dielectric performance analysis of laboratory aged power cable under harmonic voltages

Cihat Cagdas Uydur<sup>1</sup> · Oktay Arikan<sup>2</sup>

Received: 24 December 2021 / Accepted: 16 July 2022 / Published online: 7 August 2022  
© The Author(s), under exclusive licence to Springer-Verlag GmbH Germany, part of Springer Nature 2022

## Abstract

In recent years, due to the increasing use of nonlinear loads, the level of harmonics deteriorating the power quality has also increased in the distribution system. The harmonics have a negative effect on the behavior of equipment and materials, as they distort voltage and current waveforms of the system it is connected to. This leads to heating problems due to additional losses for the distribution system components. Due to the multitude of technical, environmental and social causes, the use of power cables, especially cross-linked polyethylene (XLPE) power cables, is increasing rapidly. In this context the problem of power system harmonics and using of XLPE power cables in distribution systems are spreading simultaneously. In this study, 60 kV overvoltage ( $5 \cdot U_0$ ) aging process was performed on 12/20.8 kV XLPE power cable samples at Yıldız Technical University High Voltage Laboratory. The dielectric parameters ( $P_K$ ,  $\tan\delta$  and  $C$ ) of the aged cable samples were measured. By using OMICRON CPC100/CP-TD1 measuring device, the effects of harmonics with different measurement voltages have been examined on underground cables. The performance of aged cables is analyzed under harmonic voltages and the results are presented. The disruptive effects created by the 3rd–5th and 7th order harmonics have been revealed.

**Keywords** Aging · Dissipation factor · Total harmonic distortion · XLPE cables

## 1 Introduction

Harmonics, which are caused by nonlinear loads and occur at frequencies that are multiples of the grid frequency, are important quality parameters for today's power systems. They cause heating in cables, increase in dielectric losses and malfunctions in the systems. Solid insulators are materials that are widely used in electrical networks, electrical equipment and substations. They are vital for power equipment as they separate the conductive parts from each other and from the ground, provide mechanical support and protect the equipment from other external influences. Material selection and insulation system design should be done meticulously for the reliability, continuity and economy of power

systems. Tests to determine parameters such as lifetime, partial discharge values, puncture strength, dissipation factor, which are of great importance for the selection of insulation material, are carried out on the basis of pure sinusoidal voltages [1]. However, power systems are not ideal. Current and voltage wave forms contain harmonic components. It should not be forgotten that the selected material will be forced by harmonic components as well as its nominal value, and when evaluating its dielectric properties, the electrical stress of the bonds between PE molecules along with the harmonic effect should also be taken into account [2, 3]. For example, it has been observed that if the voltage applied to the insulation material contains more than a certain percentage of harmonic content, the breakdown can occur even if the breakdown voltage of the relevant material is not reached [4, 5].

In a study examining harmonic distortions that contribute to the formation of electrical trees in XLPE cables, the effect of 5th order harmonics on the reduction of cable life has been clarified. In addition, the classification of the electric trees (ET) formed for harmonic and non-harmonic cases has been made [6, 7]. In another study, the effects of 3–5 and 7th order harmonics on partial discharge (PD) measurements have been revealed and the observed negative effect

✉ Cihat Cagdas Uydur  
ccagdasuydur@trakya.edu.tr

Oktay Arikan  
oarikan@yildiz.edu.tr

<sup>1</sup> Technical Sciences Vocational School, Trakya University, Edirne, Turkey

<sup>2</sup> Department of Electrical Engineering, Yıldız Technical University, Istanbul, Turkey

on the life of the cable is presented [8, 9]. Meanwhile, in the study examining the breakdown of materials by Birle used as insulation material in power cables by harmonic distortion voltage, dielectric losses were used to compare insulators [10]. In addition, the negative effects that may occur during the operation of direct current (DC) cables used in submarine power transmission have been simulated with the help of a mathematical model. Problems that may occur during operation with the resonance effect of harmonic components have been examined and it has been stated that there is a significant difference in behavior between steel armored cables and copper armored cables [11]. The effect of DC voltages overlapping with characteristic harmonics on PD activity and ET developments in DC XLPE dielectric test samples has experimentally investigated by Fard [12]. In general, it was stated that the structure of the developing electric trees and the related PD activity depends on the waveform, harmonic content and polarity of the applied measurement voltages. It is concluded that in the case of alternating voltage, the synergic effect of the accumulated field loads and the electric field exposed by the external voltage source is more likely to start an electrical tree than conditions under pure DC voltages [12, 13]. In addition to this, it has been stated that with the increase of the 3–5–7–11 and 13th total harmonic distortion (THD) ratio generated by the power electronics equipment, the partial discharge initial voltage (PDIV) value decreases and the PD amplitude value increases [14]. In a study investigating the breakdown effect of harmonics occurring at different phase angles under different voltage types on cable samples with artificial defects, it was stated that DC voltages have a distorting effect. Secondly, it was concluded that the impulse voltages came and the alternating current (AC) voltages were the last to affect the least [15, 16].

An experimental study dealing with harmonic distortion of the voltage applied to cardboard samples showed that dielectric losses are not only due to the fundamental component. It has also been shown that higher order harmonic components play a major role in these losses. It has been suggested that this effect may be related to the polar character of water molecules, which are heavily involved in heat dissipation [17]. Apart from this, the samples created using XLPE insulation were aged at 80 °C for 90 h and breakdown strength measurements were made with voltage that has harmonic distortion. In the study where life of cable samples is compared for harmonic and non-harmonic situations, it was emphasized that influence of harmonic should be taken into account in the design phase of insulation systems [18, 19]. In another study, the errors caused by the voltage distorted by harmonic orders in dielectric losses evaluated at operating frequencies were examined. Based on the measurement results performed on epoxy samples, it has been tried to determine the effects of harmonics. In addition, the error rates

on the measurement results of 3rd–5th–7th order harmonic distortion were shared. In addition, breakdown voltage of XLPE and epoxy resin samples is investigated. It has been revealed that harmonics negatively affect the breakdown voltages of insulating materials commonly used in cable systems [20, 21]. In a study conducted in 2021 by Linde, dielectric losses of epoxy polymer (EP) and functionally filled silicon rubber (f-SiR) samples were examined under harmonic distorted voltages and accordingly in terms of heat source density within the material. The results show that epoxy polymer samples behave linearly depending on the electric field strength and therefore allow good predictability of dielectric losses. The f-SiR samples that are examined exhibit a nonlinear behavior when an electric field threshold is exceeded. Direct loss measurements under voltage with harmonic distortion reveal a sharp increase in dielectric loss with increasing electric field strength [22].

Many studies in which overvoltage aging process is performed with 3–4–5 times the rated voltage in different aging processes have contributed to the literature in recent years. In these studies, the changing of the mechanical and dielectric parameters of the cables were investigated [23–27]. As a result of the literature review, it has been revealed that it is critical to examine the effect of overvoltages in grid on power cables under harmonic voltages. For this reason, the dielectric performance of power cables that have been aged with overvoltage should be examined. In light of BS EN 60,071, IEEE 1407 Guide and HD 605 standards, the aging process has been established in line with the laboratory facilities and the sustainability of the tests, taking into account the studies in the literature [28–31]. In this context, 12/20.8 kV XLPE power cable samples were aged using 60 kV overvoltage ( $5 \cdot U_0$ ) at Yıldız Technical University High Voltage Laboratory. Dielectric parameter measurements were performed after each aging cycle. The dielectric parameters ( $P_K$ ,  $\tan\delta$  and  $C$ ) of the aged cable samples were measured. By using OMICRON CPC100/CP-TD1 measuring device, the effects of harmonics with different measurement voltages have been examined. The performance of aged cables is analyzed under harmonic voltages and the results are presented. The disruptive effects created by harmonics have been revealed.

## 2 Theory of study

In this section, the relationship between theoretical knowledge and measurements is emphasized. First, harmonic distortion has defined. Afterward, theoretical calculations about the effect of harmonic distortion on dielectric parameters of cable are specified.

### 2.1 Harmonic distortion

Today, harmonics, whose negative effects are increasing in power systems, are defined as periodic waveform components of the grid current and voltage at multiples of the fundamental frequency. Harmonics distort current and voltage waveforms in distribution systems. The main harmonic sources are listed as devices using semiconductor elements, arc furnaces, welding machines, converters, drivers, lighting elements working with the gas discharge principle, etc. They cause problems such as waveform distortion, voltage drop, control and measurement errors, malfunctioning of elements, loss, heating, insulation stress and shortening of life in the systems they are in [32]. In power systems, you can see the instantaneous values of voltage and current without harmonic components in Eqs. 1 and 2. Equation 3 describes  $\omega$  which depends on the grid frequency.

$$v(t) = \sqrt{2} \cdot V \cdot \sin(\omega t + \varphi) \tag{1}$$

$$i(t) = \sqrt{2} \cdot I \cdot \sin(\omega t + \delta) \tag{2}$$

$$\omega = 2 \cdot \pi \cdot f \tag{3}$$

Here, "V" is the effective voltage value (V), "I" is effective value of current (A), " $\varphi$ " and " $\delta$ " are the phase angle ( $^\circ$ ), "f" is the frequency of distribution system (Hz). Although many diagnostic and testing methods are available for the examination of an electrical insulating material, the effect of harmonics is often neglected. However, insulating materials are also challenged by harmonic components in practice and their dielectric properties can change at different frequency values. Harmonics have disruptive effect on voltage and current as you can see in Eqs. 4 and 5.

$$v(t) = \sqrt{2} \cdot V_1 \cdot \sin(\omega t + \varphi_1) + \sqrt{2} \cdot V_3 \cdot \sin(3\omega t + \varphi_3) + \dots + \sqrt{2} \cdot V_i \cdot \sin(i\omega t + \varphi_i) \tag{4}$$

$$i(t) = \sqrt{2} \cdot I_1 \cdot \sin(\omega t + \delta_1) + \sqrt{2} \cdot I_3 \cdot \sin(3\omega t + \delta_3) + \dots + \sqrt{2} \cdot I_i \cdot \sin(i\omega t + \delta_i) \tag{5}$$

Here, " $V_1$ " is effective value of voltage at mains frequency (V), " $i$ " is harmonic order, " $V_i$ " is effective value of voltage at harmonic frequency of the order  $i$  (V), " $I_1$ " is effective value of current at mains frequency (A), " $I_i$ " is effective value of current at harmonic frequency of the order  $i$  (A). Therefore, the performance of insulating materials at different harmonic contents should be investigated and this performance should be taken into account when choosing materials. The main quantities used in the determination of harmonic limits are defined as total harmonic distortion (THD) and total demand

distortion (TDD) in the relevant standards and regulations [33, 34]. THD of a voltage waveform with harmonic content is expressed by Eq. 6 below. In addition, TDD associated with the current is given in Eq. 7 [32].

$$\%THD = \frac{\sqrt{\sum_{i=2}^n V_i^2}}{V_1} \cdot 100 \tag{6}$$

$$\%TDD = \frac{\sqrt{\sum_{i=2}^n I_i^2}}{I_L} \cdot 100 \tag{7}$$

Here,  $I_L$  is maximum demand load current at fundamental frequency component and " $n$ " is content of highest harmonic component in the distribution system (it is recommended to take 50) [33].

### 2.2 Effect of harmonics on dielectric parameters of power cable

Insulation materials do not actually behave ideally and pass a small amount of current through them. As a result of the current flowing on the insulation material, active power losses occur and turn into heat energy. In the studies in the literature, it is seen that the dielectric parameters are examined by parallel modeling in the investigations on underground cables. In this context, theoretical information and formulations about the parallel equivalent circuit model are shared in this section [2, 6, 11]. In this case, the equivalent circuit of insulating material containing parallel resistor and capacitor can be modeled as shown in Fig. 1 [35, 36].

Here,  $R$  ( $\Omega$ ) is the resistance representing dielectric losses,  $C$  (F) is the capacitance of insulation,  $U$  (V) is the voltage applied,  $I_R$  (A) is the current causing dielectric losses,  $I_C$  (A) is the current flowing through  $C$ ,  $I$  (A) is the total current flows through insulation and  $\delta$  ( $^\circ$ ) is the phase angle between  $I_C$  and  $I$ . Using parallel equivalent circuit parameters, dissipation factor ( $\tan \delta$ ) and dielectric losses ( $P_K$ ) can be calculated as given in Eq. 8 and Eq. 9, respectively [35].

$$\tan \delta = \frac{I_R}{I_C} = \frac{\frac{U}{R}}{U \cdot \omega \cdot C} = \frac{1}{\omega \cdot R \cdot C} \tag{8}$$

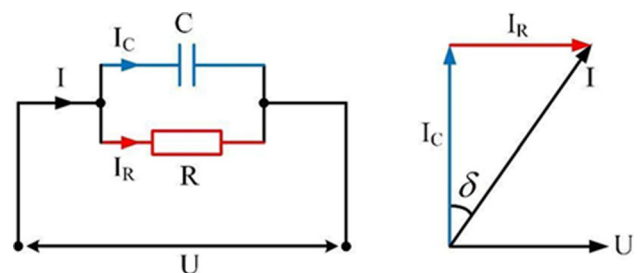


Fig. 1 Equivalent circuit and phasor diagram of insulating material

**Table 1** Parameters of cable samples

Parameter	Cable
Core type	Single
Conductor cross section (mm <sup>2</sup> )	150
Conductor material	Al
Insulation material	XLPE
Shield cross section (mm <sup>2</sup> )	25
Shield material	Cu
Sample length (m)	5

$$P_k = \omega \cdot C \cdot U^2 \cdot \text{Tan}\delta \quad (9)$$

However, if there is harmonic content in the system, harmonic components should also be added to  $\text{tan}\delta$  and dielectric loss calculation. Calculations of the power loss ( $P_K$ ) and  $\text{tan}\delta$  parameters belong to each harmonic component are shown in Eqs. 10 and 11. Here,  $i$  is harmonic order.

$$\text{Tan}\delta = \frac{I_R}{I_C} = \frac{\frac{U_i}{R}}{U_i \cdot i \cdot \omega \cdot C} = \frac{1}{i \cdot \omega \cdot R \cdot C} \quad (10)$$

$$P_{Ki} = i \cdot \omega \cdot C \cdot U_i^2 \cdot \text{Tan}\delta \quad (11)$$

Another dielectric loss element in insulating materials is polarization. When an alternating electric field is applied to the material, the charge dipoles change direction every half cycle and move in the opposite direction. The frequency of this movement is determined by the frequency of the applied voltage and the losses caused by infiltration during the operation are called polarization losses. After a threshold frequency value, at very high frequencies where the voltage half-wave lasts for a very short time, the dipoles cannot follow the electric field and cannot change their position with respect to the field. In other words, with the frequency, polarization losses increase up to a point and decrease after a point [35].

### 3 Experimental setup

In this section, detailed information about the preparation of the cable samples, the properties of the aging process and the measurement system have shared in the experimental studies carried out in High Voltage Laboratory of Yıldız Technical University. In the experimental study, cable samples with 12/20.8 kV rated voltage had used. Detailed information on the parameters of the cable samples have stated in Table 1.

Considering the laboratory facilities and the sustainability of the tests, the samples has aged with overvoltage by 15 min intervals, five times the rated voltage ( $5 \cdot U_0$ ) using the test

set-up given in Fig. 2.  $5 \cdot U_0$  overvoltage at 50 Hz frequency was applied to the cable insulation with the help of a variac connected to the primary of the 220 V/100 kV, 10 kVA high voltage test transformer. In order to ensure measurement consistency and reliability, three samples were prepared from the specified cable and overvoltage aging process was performed for each sample. Laboratory test setup prepared for aging and dielectric measurements are shown in Figs. 2 and 3.

Before starting the aging process, dielectric parameters of three unaged cable samples had been measured and thereafter, dissipation factor ( $\text{tan}\delta$ ), capacitance ( $C_p$ ), dielectric losses ( $P_K$ ) and resistance ( $R_p$ ) had been measured after each 15 min aging cycle. As seen in Fig. 3, dielectric measurements were carried out by Omicron CPC100/CP-TD1 device during all cycles of aging. Measurement sensitivities of the device are shown in Table 2 [36]. Here,  $I_x$  defines current during capacitance measurement.

The high voltage probe of the device is connected to the cable conductor and the measurement probe to the cable shield. The device can measure with a frequency of 50–400 Hz and a range of 2–12 kV. Thus, changes of dielectric parameters at different frequencies (Hz) and voltages (kV) could examined and the working range with the greatest change was determined. For this, measurements in each cycle were carried out separately at 2, 4, 6, 8, 10 and 12 kV. 50, 100, 150, 200, 250, 300, 350 and 400 Hz are used as the measurement frequency for each of these voltages. The effects of frequency and voltage changes were investigated by obtaining  $R_p$ ,  $\text{tan}\delta$ ,  $C_p$  and  $P_K$  measurement results in 2–12 kV and 50–400 Hz intervals with 2 kV and 50 Hz steps. Electrical parameters ( $\text{tan}\delta$ ,  $P_k$ ,  $C_p$  and  $R_p$ ) of cable insulation are related to the test temperature. For this reason, laboratory ambient temperature is recorded during the measurements as  $25 \pm 2$  °C.

## 4 Measurement results

In this section, the measurement results of dielectric parameters made at different voltages and frequencies are presented depending on the number of aging cycles. The measurement results have been evaluated under a separate heading for each dielectric parameter, about  $P_K$ ,  $\text{tan}\delta$ ,  $C_p$  and  $R_p$  by taking the average of cable samples.

### 4.1 Dielectric losses ( $P_K$ )

$P_K$  measurement results and data were analyzed depending on frequency and voltage to examine the effect of aging in cables. As can be seen in Fig. 4, it is seen that a cable sample with 12 kV rated voltage, which is aged with overvoltage, has increased by 10% in the  $P_K$  increase since the first aging.



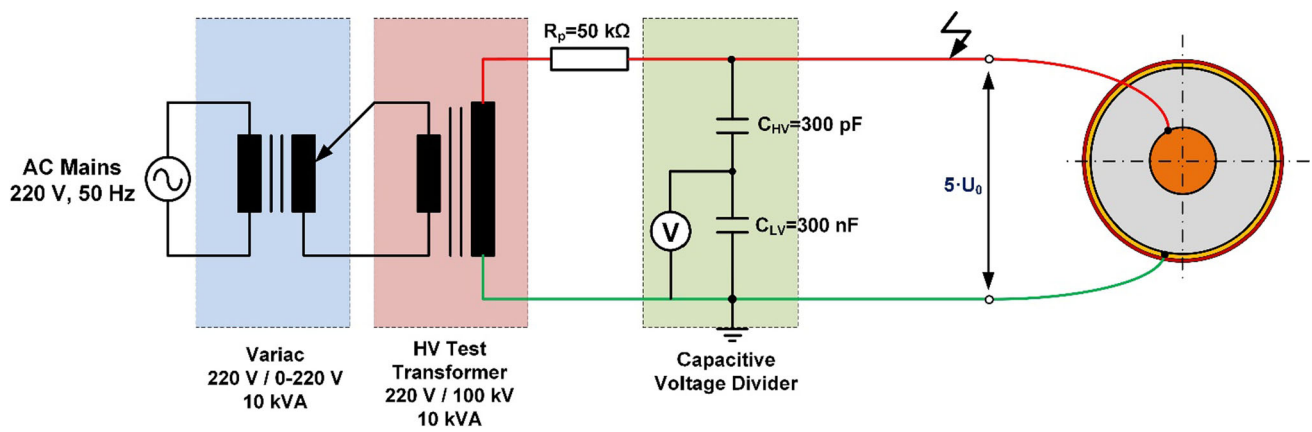


Fig. 2 Schematic representation of experimental test set-up used for overvoltage aging

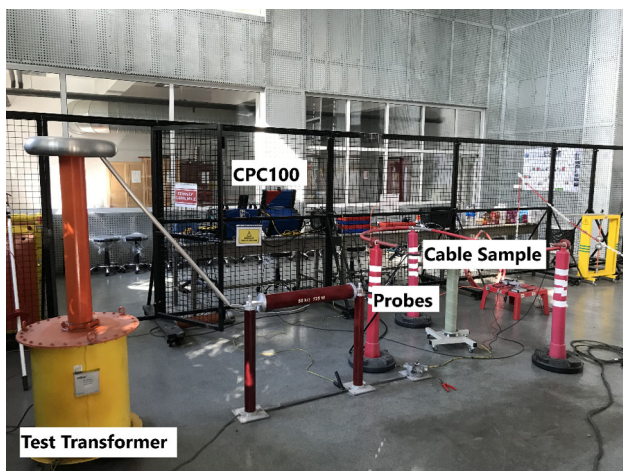


Fig. 3 Laboratory test set-up

The negative effects of overvoltage on the cable have continued throughout 80 aging process. The data tables contain all frequency data of the cable sample at rated voltage and all voltage data at rated frequency.

Figure 4a shows the results of  $P_K$  measurements made at a voltage of 12 kV in the frequency range 50–400 Hz. When the measurements made before the aging process were compared with the measurements after the 80th aging cycle, an increase of 181.4% at 50 Hz, 150% at 100 Hz, 132% at 150 Hz, 118% at 200 Hz, and 105% at 250 Hz. This ratio was observed as 91.5% at 300 Hz, 78.5% at 350 Hz and 67.5% at 400 Hz. It has been revealed that the  $P_K$  values increasing as the Watt value

with the increase in frequency exhibit different behaviors as the percentage increase amount. All measurement data, according to frequency, are presented in detail in Table 3, with 10 aging cycles each. Figure 4b shows the results of  $P_K$  measurements made at a frequency of 50 Hz in the voltage range of 2–12 kV. When the measurements made in the 80th aging cycle are compared according to the cable condition before aging, 98.4% at 2 kV voltage, 130% at 4 kV voltage, 146.6% at 6 kV voltage, 160.6% at 8 kV voltage, 169.5% at 10 kV voltage, 181.4% at 12 kV voltage, rate increased. It has been observed that the  $P_K$  in the cable increase with the increase in the measuring voltage. All measurement data, according to voltage, are presented in detail in Table 4.

In the pre-aging measurements in Table 3, according to the value of the  $P_K$  value at 50 Hz; 56.2% at 100 Hz, 104% at 150 Hz, 146.3% at 200 Hz, 186.5% at 250 Hz, 228.7% at 300 Hz, 271.4% at 350 Hz, and 400 Hz It was observed that it increased by 321.3%. After 80 aging processes, the increase rates for 100–150–200–250–300–350–400 Hz frequency values changed as 38.8%–68.4%–90.8%–108.5%–123.8%–135.7–150.9%, respectively. When the pre-aging measurements in Table 4 are examined, according to the value of  $P_K$  at 2 kV voltage; it is seen that it increases by 819.3% at 6 kV and by 3432.5% at 12 kV. After 80 aging processes, the increase rates for 6 kV and 12 kV voltage values changed as 1042.7–4909.7%, respectively.

Table 2 CPC100/ CP-TD1 measuring sensitivity

Parameter	Range	Resolution	Typical accuracy	Conditions
$C$	1 pF.....3 μF	6 digits	Error < 0.2% of reading	$I_x > 8 \text{ mA}$ $V_{\text{test}} = 300 \text{ V}..... 10 \text{ kV}$
$\tan\delta$	0 ..... 100 (0 ..... 10,000%)	5 digits	Error < 0.5% of reading + 0.02%	$V_{\text{test}} = 300 \text{ V}..... 10 \text{ kV}$

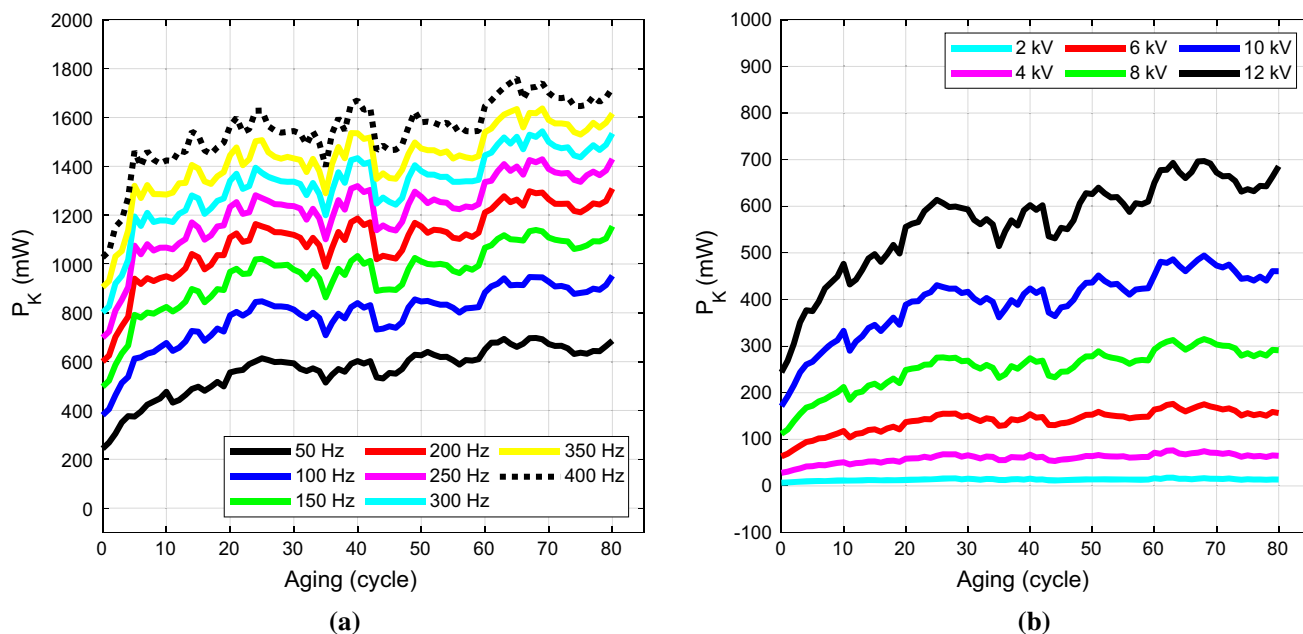


Fig. 4  $P_K$  measurements results due to aging: a at 12 kV, b at 50 Hz

Table 3  $P_K$  (mW) measurement data for changing frequency at 12 kV voltage

Aging cycle	$P_K$ (mW)							
	50 Hz	100 Hz	150 Hz	200 Hz	250 Hz	300 Hz	350 Hz	400 Hz
0	243.7	380.7	497.3	600.2	698.4	801.2	905.3	1027.0
10	476.3	676.3	823.8	949.5	1067.0	1178.0	1284.2	1424.3
20	555.7	789.7	967.8	1108.9	1234.0	1340.7	1445.5	1564.7
30	593.0	813.2	976.7	1119.3	1237.0	1337.1	1432.3	1544.5
40	602.3	839.8	1032.4	1186.1	1318.9	1433.3	1535.5	1670.1
50	626.2	846.5	1010.3	1153.8	1275.6	1380.5	1473.0	1580.3
60	650.3	883.4	1066.4	1210.8	1335.6	1445.0	1540.0	1646.8
70	672.4	927.6	1108.3	1265.3	1389.3	1500.0	1589.8	1701.3
80	685.8	952.0	1154.6	1308.7	1430.3	1534.6	1616.2	1720.7
Rate of change	%181.4	%150.1	%132.2	%118.0	%104.8	%91.5	%78.5	%67.5

Table 4  $P_K$  (mW) measurement data for changing voltage at 50 Hz frequency

Aging cycle	$P_K$ (mW)					
	2 kV	4 kV	6 kV	8 kV	10 kV	12 kV
0	6.9	28.1	63.4	111.7	171.0	243.7
10	11.8	50.8	117.8	212.1	332.6	476.3
20	13.1	58.4	137.0	248.8	388.7	555.7
30	15.5	65.7	150.9	268.7	416.5	593.0
40	15.6	67.0	153.9	273.9	423.6	602.3
50	13.8	64.0	152.9	278.1	436.4	626.2
60	16.5	71.2	163.8	292.8	451.8	650.3
70	15.3	70.9	167.7	303.4	472.9	672.4
80	13.7	64.6	156.4	291.1	460.7	685.8
Rate of change	%98.4	%129.9	%146.6	%160.6	%169.4	%181.4

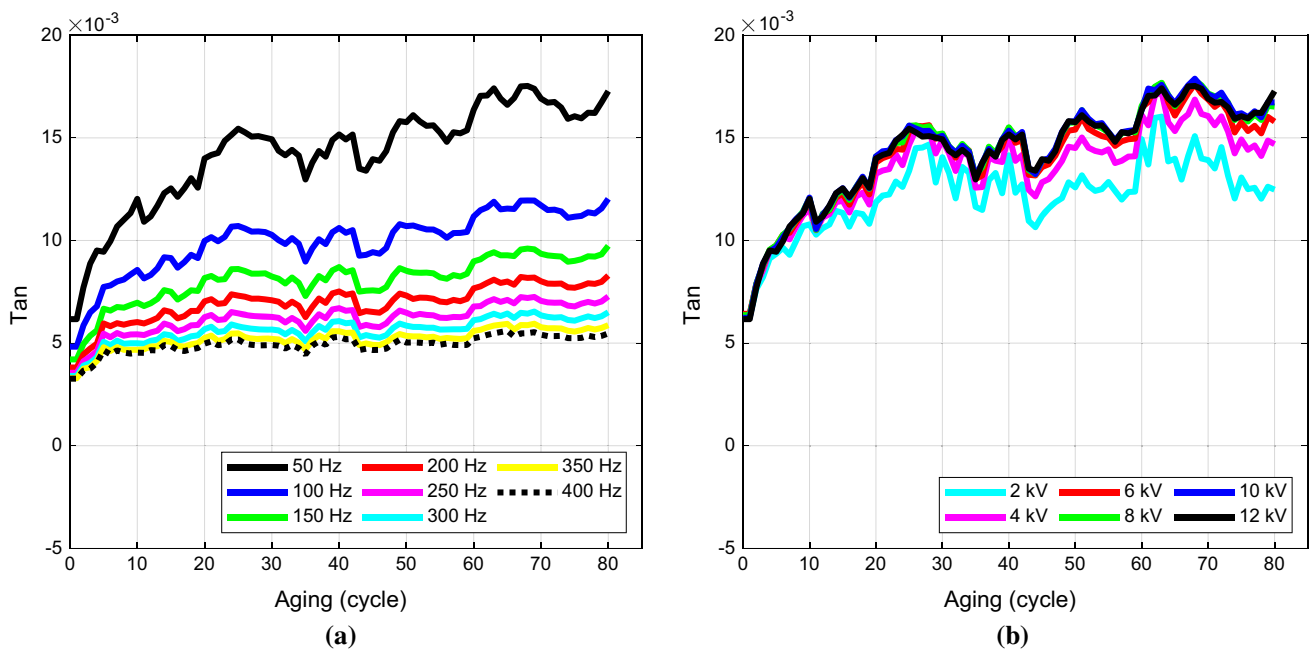


Fig. 5  $\tan\delta$  measurements results due to aging: **a** at 12 kV, **b** at 50 Hz

### 4.2 Dissipation factor ( $\tan\delta$ )

In this section,  $\tan\delta$  measurement results and data, which allow us to evaluate the insulation quality of the cable, are examined depending on frequency and voltage, in order to examine the negative effect of overvoltage on XLPE cables. In Fig. 5, which is formed due to aging; Fig. 5a shows the results of  $\tan\delta$  measurements made at 12 kV in the frequency range of 50–400 Hz, and Fig. 5b shows the measurement results at 50 Hz in the voltage range of 2–12 kV.

When the measurement results were examined, it was observed that the increase in  $\tan\delta$  value at 50–400 Hz measurement frequency as a result of 80 aging processes was 180%—149%—132%—118%—105%—91%—78%—67%, respectively. It is seen that as the number of aging cycles increases,  $\tan\delta$  value increases, but as the frequency increases, the rate of increase in the measurement results decreases. This situation indicates that measurements made at different frequencies reveal the harmonic effect and frequency-dependent changes should be examined in detail. The data of the measurement results are shared in Table 5, including 10 aging cycles in the frequency range of 50–400 Hz. In Fig. 5b; the rate of increase in  $\tan\delta$  measured between 2 and 12 kV after the 80th aging cycle was 98% at 2 kV, 129% at 4 kV, 146% at 6 kV, 161% at 8 kV, at 10 kV 171.2% and 180.2% at 12 kV. All measurement data, according to voltage, are presented in detail in Table 6, with

10 aging cycles. In this context, it was observed that  $\tan\delta$  and  $P_K$  values showed similar characteristics.

In the pre-aging measurements in Table 5, according to the value of  $\tan\delta$  at 50 Hz; 21.7% at 100 Hz, 31.8% at 150 Hz, 38.2% at 200 Hz, 42.4% at 250 Hz, 44.9% at 300 Hz, 46.6% at 350 Hz, and 400 Hz It is seen that it decreased by 47%. After 80 aging processes, the decrease rates for 100–150–200–250–300–350–400 Hz frequency values changed as 30.4%–43.6%–52%–57.9%–62.4%–66%–68.3%, respectively.

When the pre-aging measurements in Table 6 are examined, according to the  $\tan\delta$  value at 2 kV voltage; it is seen that it changes by 2% at 6 kV and 12 kV. In the measurements made after the 80 aging process, the  $\tan\delta$  value increased by 26.6%–38.5% for the 6 kV and 12 kV voltage values, respectively.

### 4.3 Cable capacitance ( $C_p$ )

The measurement results of the  $C_p$  value, which has a very important place in the reactive power balance and allows us to examine the capacitive behavior of cables due to aging, depending on voltage and frequency are presented in Fig. 6. The data of the measurement results are shared in Table 7, including 10 aging cycles in the frequency range of 50–400 Hz and measurement data, according to voltage, are presented in detail in Table 8.

**Table 5** Tan $\delta$  measurement data for changing frequency at 12 kV voltage

Aging cycle	tan $\delta$							
	50 Hz	100 Hz	150 Hz	200 Hz	250 Hz	300 Hz	350 Hz	400 Hz
0	0.0062	0.0048	0.0042	0.0038	0.0036	0.0034	0.0033	0.0033
10	0.0120	0.0086	0.0070	0.0060	0.0054	0.0050	0.0047	0.0045
20	0.0140	0.0100	0.0082	0.0070	0.0063	0.0057	0.0053	0.0050
30	0.0149	0.0103	0.0082	0.0071	0.0063	0.0057	0.0052	0.0049
40	0.0152	0.0106	0.0087	0.0075	0.0067	0.0061	0.0056	0.0053
50	0.0158	0.0107	0.0085	0.0073	0.0065	0.0059	0.0054	0.0050
60	0.0164	0.0112	0.0090	0.0077	0.0068	0.0061	0.0056	0.0052
70	0.0169	0.0117	0.0094	0.0080	0.0071	0.0064	0.0058	0.0054
80	0.0173	0.0120	0.0097	0.0083	0.0073	0.0065	0.0059	0.0055
<b>Rate of change</b>	%180.2	%149.3	%131.6	%117.5	%104.7	%91.4	%78.5	%67.5

**Table 6** Tan $\delta$  Measurement Data for Changing Voltage at 50 Hz Frequency

Aging cycle	tan $\delta$					
	2 kV	4 kV	6 kV	8 kV	10 kV	12 kV
0	0.0063	0.0064	0.0064	0.0064	0.0062	0.0062
10	0.0108	0.0115	0.0119	0.0121	0.0121	0.0120
20	0.0119	0.0133	0.0138	0.0141	0.0141	0.0140
30	0.0141	0.0149	0.0152	0.0152	0.0151	0.0149
40	0.0141	0.0152	0.0155	0.0155	0.0154	0.0152
50	0.0126	0.0145	0.0154	0.0158	0.0158	0.0158
60	0.0149	0.0161	0.0165	0.0166	0.0164	0.0164
70	0.0139	0.0161	0.0169	0.0172	0.0171	0.0169
80	0.0125	0.0147	0.0158	0.0165	0.0167	0.0173
<b>Rate of change</b>	%98.3	%129.2	%145.7	%159.6	%168.5	%180.2

When the data of the measurement results were examined, it was shown that the  $C_p$  value did not change depending on aging. This is observed in all variations with measuring frequency and measuring voltage. In this context, the negligibility of the changes in the  $C_p$  value is among the results obtained.

When the measurement results of  $C_p$  are examined, it is seen that the changes in  $C_p$  values are between 0.4 and 1% after all aging cycles. Considering that the measured size is on the pico level, it becomes evident that these rates of change can be neglected. It has been observed that the  $C_p$  value behaves independently of the measurement voltage and measurement frequency.

#### 4.4 Resistance ( $R_p$ )

In this section, resistance ( $R_p$ ) value measurement results from cable parameters are shared. When the measurement

results of  $R_p$  are examined, it has been observed that the  $R_p$  value showed inversely behavior with the  $P_K$  value as expected.

Figure 7a shows the results of  $R_p$  measurements made at a voltage of 12 kV in the frequency range 50–400 Hz. When the measurements made before the aging process were compared with the measurements after the 80th aging cycle, a decrease of 90.3% at 50 Hz, 86.5% at 100 Hz, 83.6% at 150 Hz, 79.6% at 200 Hz, and 75.2% at 250 Hz. This ratio was observed as 72.9% at 300 Hz, 70.7% at 350 Hz and 65.9% at 400 Hz. It has been revealed that the  $R_p$  values decreasing as the  $M\Omega$  value with the decrease in frequency exhibit different behaviors as the percentage decrease amount. All measurement data, according to frequency, are presented in detail in Table 9, with 10 aging cycles each.

Figure 7b shows the results of  $R_p$  measurements made at a frequency of 50 Hz in the voltage range of 2–12 kV. When the measurements made in the 80th aging cycle are compared



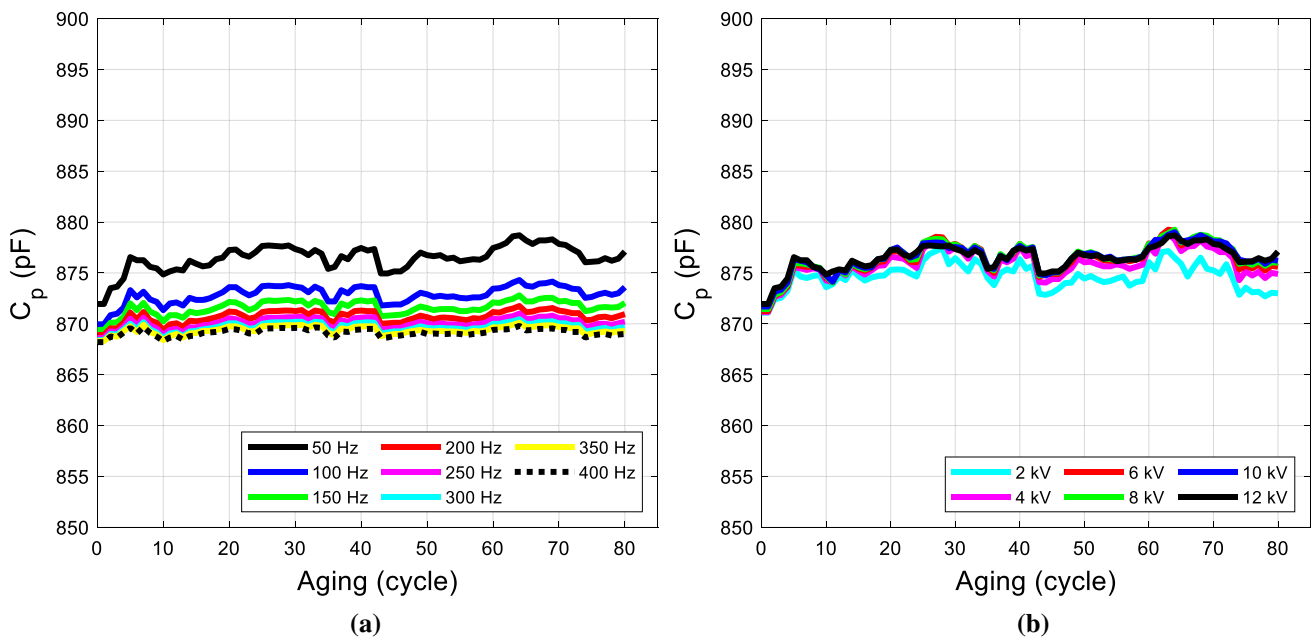


**Fig. 6**  $C_p$  measurements results due to aging: **a** at 12 kV, **b** at 50 Hz

**Table 7**  $C_p$  (pF) measurement data for changing frequency at 12 kV voltage

Aging cycle	$C_p$ (pF)							
	50 Hz	100 Hz	150 Hz	200 Hz	250 Hz	300 Hz	350 Hz	400 Hz
0	872.0	870.0	869.4	868.9	868.6	868.4	868.3	868.2
10	874.9	871.4	870.3	869.4	868.9	868.6	868.4	868.3
20	877.3	873.6	872.2	871.2	870.6	870.1	869.8	869.5
30	877.4	873.7	872.2	871.3	870.7	870.2	869.9	869.6
40	877.5	873.7	872.3	871.3	870.6	870.1	869.8	869.5
50	876.8	872.9	871.6	870.7	870.1	869.6	869.3	869.0
60	877.5	873.5	872.1	871.2	870.5	870.0	869.7	869.4
70	877.9	873.8	872.2	871.3	870.6	870.1	869.7	869.4
80	877.1	873.6	872.1	871.0	870.2	869.7	869.3	869.0
Rate of change	%0.6	%0.4	%0.3	%0.2	%0.2	%0.1	%0.1	%0.1

**Table 8**  $C_p$  (pF) measurement data for changing voltage at 50 Hz frequency

Aging cycle	$C_p$ (pF)					
	2 kV	4 kV	6 kV	8 kV	10 kV	12 kV
0	871.1	871.2	871.3	871.5	871.7	872.0
10	873.6	874.3	874.5	874.7	874.8	874.9
20	875.3	876.6	877.1	877.3	877.3	877.3
30	876.5	877.5	877.9	877.8	877.6	877.4
40	876.4	877.6	877.9	877.9	877.7	877.5
50	874.5	876.1	876.7	876.9	876.9	876.8
60	876.1	877.6	877.9	877.9	877.5	877.5
70	875.3	877.5	878.2	878.3	878.1	877.9
80	873.0	874.9	875.6	876.0	876.2	877.1
Rate of change	%0.2	%0.4	%0.5	%0.5	%0.5	%0.6

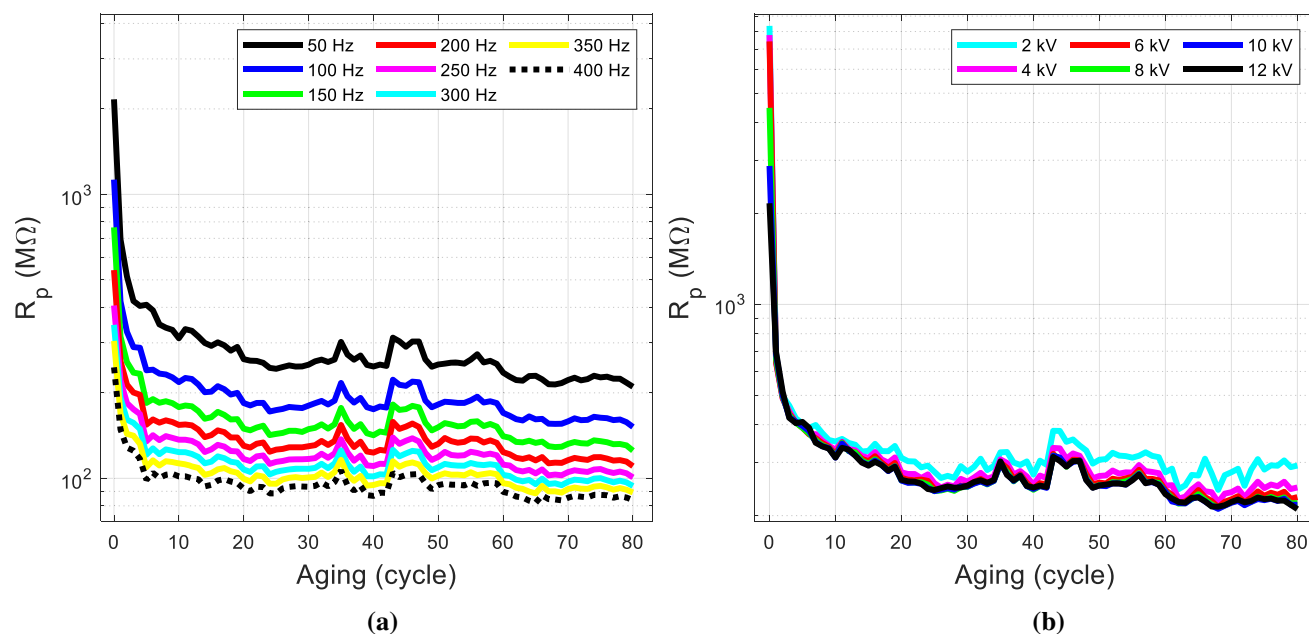


Fig. 7  $R_p$  measurements results due to aging: **a** at 12 kV, **b** at 50 Hz

according to the cable condition before aging, 96.5% at 2 kV voltage, 96.8% at 4 kV voltage, 96.9% at 6 kV voltage, 95.1% at 8 kV voltage, 92.4% at 10 kV voltage, 90.3% at 12 kV voltage, rate decreased.

The data of the measurement results are shared in Table 9, including 10 aging cycles in the frequency range of 50–400 Hz and measurement data, according to voltage, are presented in detail in Table 10. Considering Eq. 10 and 11, it is clearly seen that the changes in  $R_p$  values are complementary to the measurement results. In the pre-aging measurements in Table 9, according to the value of  $R_p$  at 50 Hz; it is seen that it decreased by 47.9% at 100 Hz, 64.6% at 150 Hz, 75% at 200 Hz, 81.2% at 250 Hz, 84% at 300 Hz, 86% at 350 Hz, and 400 Hz, 88.6%. After 80 aging processes, the decrease rates for 100–150–200–250–300–350–400 Hz frequency values changed as 27.8%–40.4%–47.5%–52%–55.3%–57.6%–60.1%, respectively. When the pre-aging measurements in Table 10 are examined, according to the value of  $R_p$  at 2 kV voltage; it is seen that it increased by 11.2% at 6 kV and by 74.1% at 12 kV. After 80 aging processes, the increase rates for 6 kV and 12 kV voltage values changed as 21.4%–28.3%, respectively.

It is seen that the resistance value decreases with increasing frequency, and the current increases with increasing measuring voltage, so the dielectric loss values, which are directly proportional to the square of the current, increase. It has been determined that the dielectric performance is dosed by affecting the cable impedance due to harmonic orders. The reason for this increase in the beginning phase of the aging process is that the bonds between PE molecules are

exposed to electrical stress, which leads to them becoming stretched, and results in dielectric losses. As the frequency is increased, the vibrational movements due to the electric field on atomic and molecular basis also increase [3, 26, 37].

## 5 Discussion

In this section, in order to examine the behavior of measurement results of the pre-aging and 80th aging cycles, the gradient of data is specified in figures created depending on the frequency and voltage. In addition, evaluations were made on data of 10 aging cycles and it was interpreted which harmonic component had more negative effects on cable at which voltage.

### 5.1 Dielectric losses (PK)

In Fig. 8,  $P_K$  measurement results for pre-aging and post-80 aging are shared. Figure 8a is frequency dependent at 12 kV measuring voltage, while Fig. 8b shows the data in voltage dependent form at 50 Hz frequency.

While the gradient of the frequency-dependent measurement data was calculated as 2.1704 before aging, this value increased to 2.8159 after the 80th aging. In this context, it reveals that the gradient of the  $P_K$  value increases at different frequency values and that the harmonic components affect the aging of the cable. Although the gradient of the pre-aging data was 23.7291 in the  $P_K$  value examined depending on the stress, it was found that this value was 66.9056 after 80 aging cycles. Thus, the negative effect of voltage on  $P_K$  is clearly

**Table 9**  $R_p$  (M $\Omega$ ) Measurement Data for Changing Frequency at 12 kV Voltage

Aging cycle	$R_p$ (M $\Omega$ )							
	50 Hz	100 Hz	150 Hz	200 Hz	250 Hz	300 Hz	350 Hz	400 Hz
0	2161.5	1127.1	765.3	541.1	406.1	347.1	304.7	246.0
10	311.4	218.2	178.2	154.2	136.8	123.7	112.9	101.6
20	262.8	184.1	149.6	130.2	116.9	107.4	99.6	92.0
30	251.3	180.3	149.0	129.7	117.0	108.0	100.7	93.4
40	247.7	175.2	141.8	123.2	110.5	101.6	94.7	86.7
50	251.8	182.1	151.4	132.3	119.0	109.4	102.3	94.7
60	235.5	170.0	140.7	123.7	111.7	102.8	96.1	89.5
70	222.0	158.7	132.3	115.9	105.2	97.3	91.7	85.5
80	210.1	151.7	125.2	110.4	100.8	94.0	89.2	83.8
Rate of change	−%90.3	−%86.5	−%83.6	−%79.6	−%75.2	−%72.9	−%70.7	−%65.9

**Table 10**  $R_p$  (M $\Omega$ ) Measurement Data for Changing Voltage at 50 Hz Frequency

Aging cycle	$R_p$ (M $\Omega$ )					
	2 kV	4 kV	6 kV	8 kV	10 kV	12 kV
0	8353.0	7787.5	7421.0	4472.5	2872.0	2161.5
10	351.8	330.6	319.0	313.6	311.3	311.4
20	310.6	278.2	266.9	261.5	261.3	262.8
30	279.4	259.1	251.1	249.1	249.6	251.3
40	273.6	252.8	245.6	243.6	245.2	247.7
50	306.2	270.5	257.2	252.4	251.4	251.8
60	278.4	251.5	242.9	240.1	240.1	235.5
70	278.4	239.1	226.4	221.4	220.6	222.0
80	293.0	247.9	230.3	220.1	217.2	210.1
Rate of change	−%96.5	−%96.8	−%96.9	−%95.1	−%92.4	−%90.3

understood. The increasing gradient value has enabled us to understand the negative effect of the change in the effective value of the voltage on the cable due to the effect of harmonic components.

In frequency-dependent analysis of measurement data, as the number of aging cycles increases at the fundamental frequency (50 Hz), the  $P_K$  value occurring in the cable also increases. The amount of increase was determined as 95.4%–128%–143.3%–147.1%–156.9%–166.8%–175.8% and 181.4% for cycles from 10 to 80, respectively. In this context, the amount of increase between aging cycles is also very important. For example, while the  $P_K$  value increased by 128% after 20 cycles, there was an increase of 19.1% in the 40th aging cycle compared to the 20th aging. At the end of 60 cycles, an increase of 19.7% occurred compared to the 40th cycle, while an increase of 14.6% was observed in the 80th aging cycle compared to the 60th cycle. When this situation is examined in terms of harmonic component frequencies, it is revealed that the 3rd (150 Hz)

harmonic component produces the highest increase in the data analyzed every 20 cycles comparatively. The increase in  $P_K$  at 150 Hz frequency was 94.6% at the end of the first 20 aging. The 3rd component harmonic is followed by the 5th (250 Hz) and 7th (350 Hz) harmonic components, respectively. When it comes to the 40th aging cycle, the 3rd, 5th and 7th order harmonics showed a similar increase compared to the 20th aging, and this rate is 13%. At the end of 80 aging cycles, it was found that the 3rd harmonic component was the factor that most affected the  $P_K$  value.

When the voltage-dependent evaluation of the  $P_K$  data was made, it was noticed that the  $P_K$  value exhibited similar characteristics at all voltage values until the 60th aging cycle. For example, while it varies between 107 and 122% in the 20th cycle, it contains very close values between 20 and 30% in the 40th cycle. After the 60th cycle, it has been revealed that increasing voltage value is an important factor in the increase in  $P_K$ .

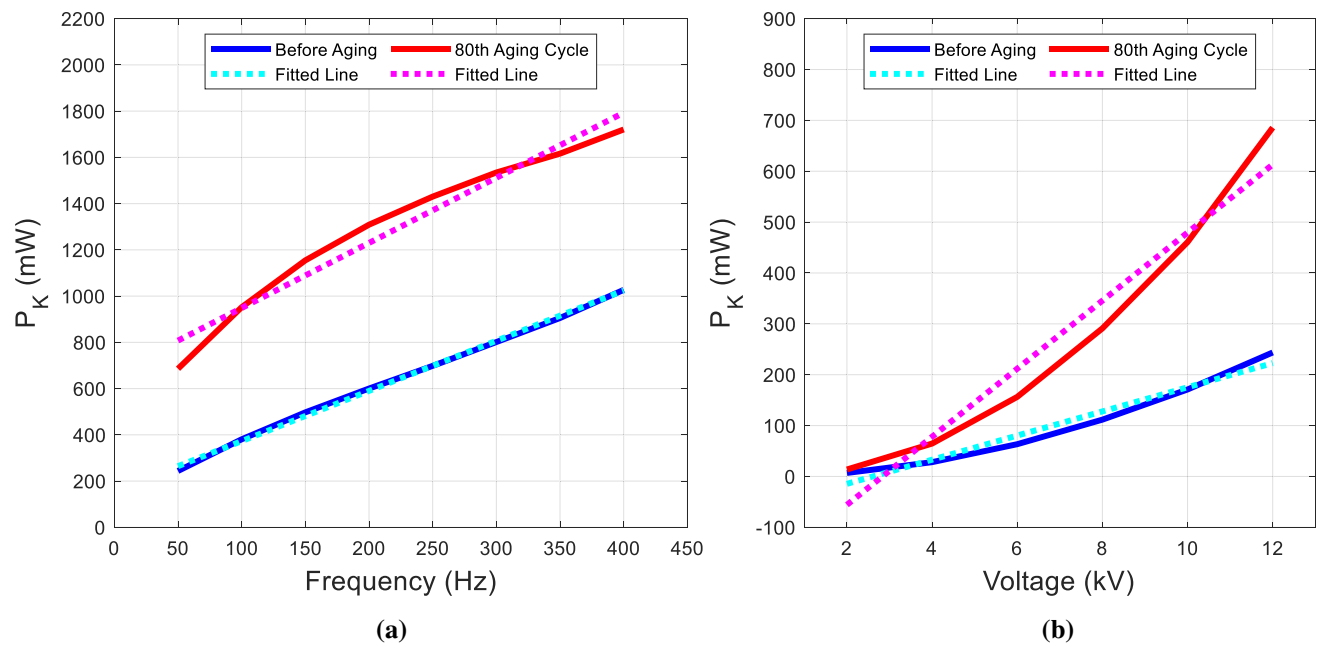


**Fig. 8** Measurements results of  $P_K$ : **a** due to frequency, **b** due to voltage

## 5.2 Dissipation factor ( $\tan\delta$ )

In Fig. 9, the change in frequency and voltage domain of the  $\tan\delta$  measurement results pre-aging and the 80th aging cycle are given and their behavior with gradient lines has been examined. The gradient of the frequency-dependent  $\tan\delta$  value was determined as  $-7.29e-06$  before aging. The negative gradient value proved its decreasing behavior. At the end of 80th aging cycle, the gradient on the frequency domain has reached the value  $-29.56e-06$ . Thus, it was revealed that the aging effect increased the amount of decrease. In addition, it has been observed that the effect of aging is not only at the rated frequency, but also the presence of a negative effect on harmonic frequencies. When the voltage dependent  $\tan\delta$  value is examined, it is determined that the gradient is  $-1.75e-05$ . Because of this value is negative, it revealed the decrease in the value of  $\tan\delta$  due to the voltage. At the end of 80th aging cycle, this value reached  $44.07e-05$ . It has been observed that with the increase in the voltage domain, the amount of increase also increased. The display of this behavior in the rated frequency depending on the voltage is an indication that more negative effects will occur as a result of the increase in the effective value of the voltage with the contribution of harmonic components.

As stated in Eq. 8,  $\tan\delta$  value decreases as the frequency increases. This situation is clearly seen when the first 20 aging cycles are examined in the measurement results. However, the rate of decrease in the  $\tan\delta$  value after the 20th cycle is around 1%. After the 40th aging cycle, the most decrease occurs in the 5th and 7th harmonic components, and this rate

is 2.7%. When the 80th cycle is reached, it is seen that the 3rd order harmonic component causes the highest decrease with 1.5%. This ratio is 0.7% for the 5th harmonic and 0.6% for the 7th harmonic. As a result, it has been revealed that 3–5–7 harmonic components have a negative effect on the  $\tan\delta$  value.

In the voltage-dependent investigations, it was observed that  $\tan\delta$  value exhibited a very similar behavior to the  $P_K$  and the increase–decrease amounts were very close to each other. There are differences between 0.5 and 0.8% of change rates. In this context, just like the  $P_K$  value, it turns out that the voltage increase is an effective factor on  $\tan\delta$ .

## 5.3 Cable capacitance ( $C_p$ )

In Fig. 10, the measurement results of the  $C_p$  value depending on the voltage and frequency are shared.

In frequency-based analysis, the gradient of  $C_p$  change before aging is  $-0.0090$ . After 80 aging cycles, the gradient value was calculated as  $-0.0205$ . It was observed that the  $C_p$  value changed inversely with the frequency and the  $C_p$  value decreased as the frequency increased. The fact that the measurement data is in the pico order indicates that the amount of change can be neglected. When the voltage-dependent  $C_p$  value was examined, the calculated gradient values were calculated as 0.0871 and 0.3543 for pre-aging and after 80th aging, respectively. In this context, it was observed that the  $C_p$  value increased with increasing voltage. Due to the small amount of increase, it was accepted that it could be ignored.

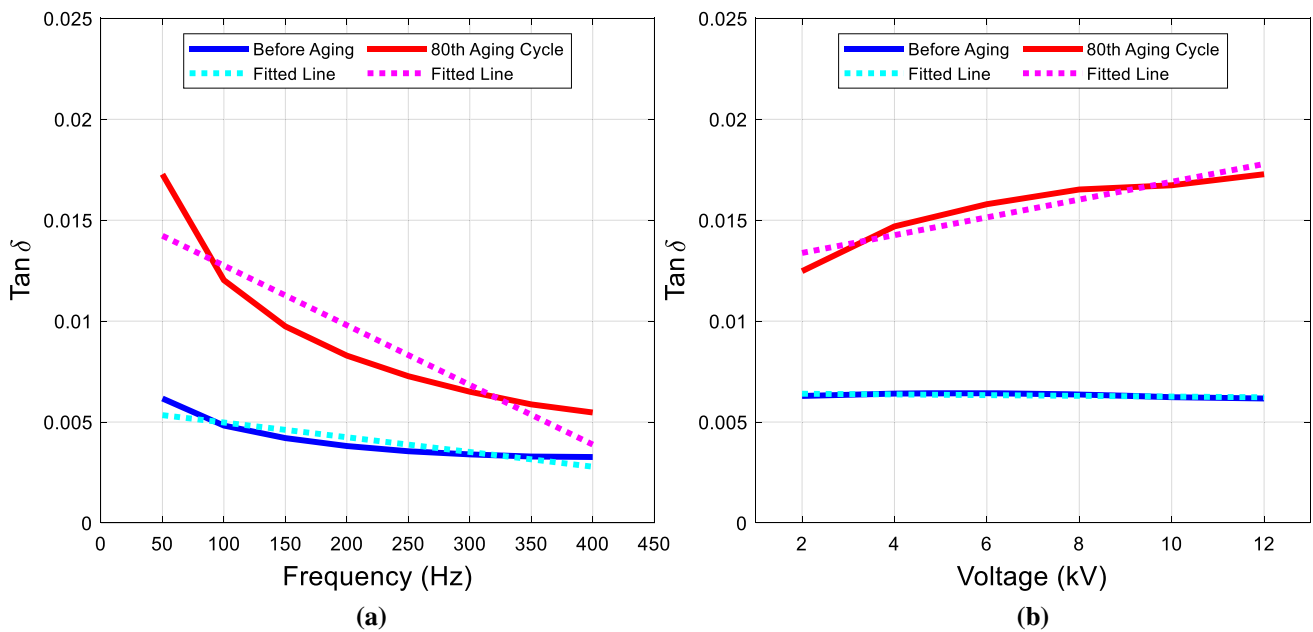


Fig. 9 Measurements results of  $\tan\delta$ : **a** due to frequency, **b** due to voltage

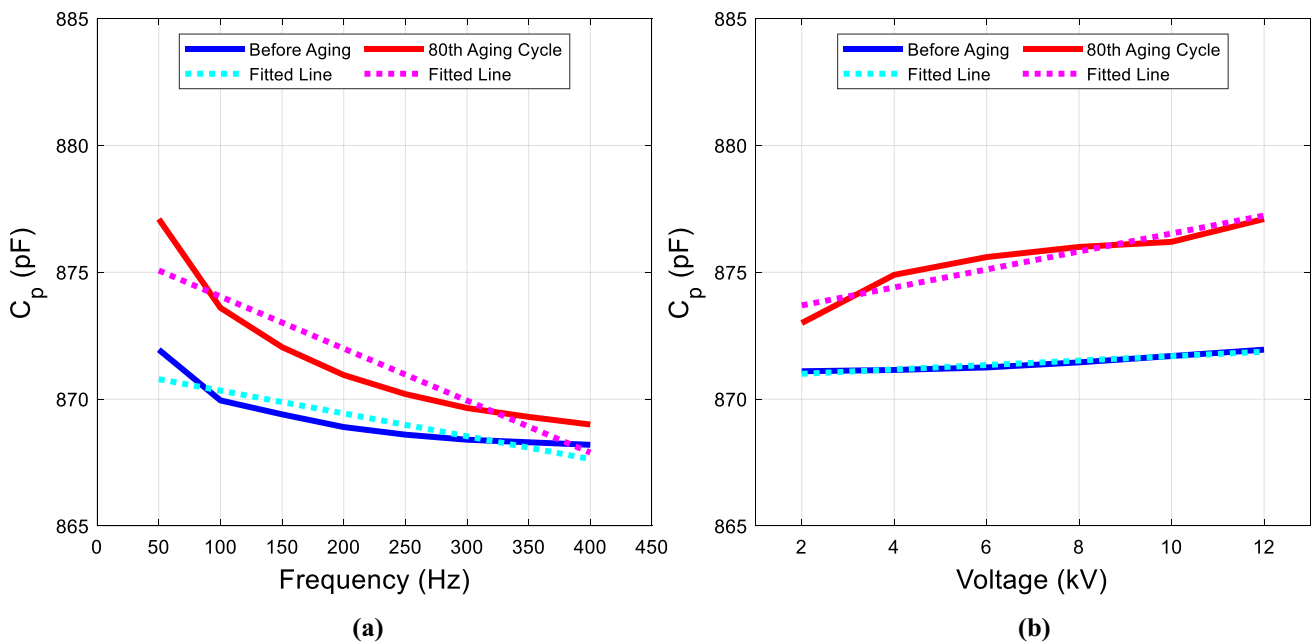


Fig. 10 Measurements results of  $C_p$ : **a** due to frequency, **b** due to voltage

In the analysis of the changes in  $C_p$  value depending on aging in voltage and frequency-dependent investigations, the rate of change was determined as 1% at most. No significant results were obtained in the comparison of the measurements made at different frequencies and the examination of the measurements made at different voltages. Considering that the measured  $C_p$  value is in the pico order, it is concluded that the change amounts can be neglected and the harmonic

components do not affect the  $C_p$  value even after the aging process.

### 5.4 Resistance ( $R_p$ )

In Fig. 11, the change in frequency and voltage domain of the  $R_p$  measurement results pre-aging and the 80th aging cycle are given and their behavior with gradient lines has been examined.



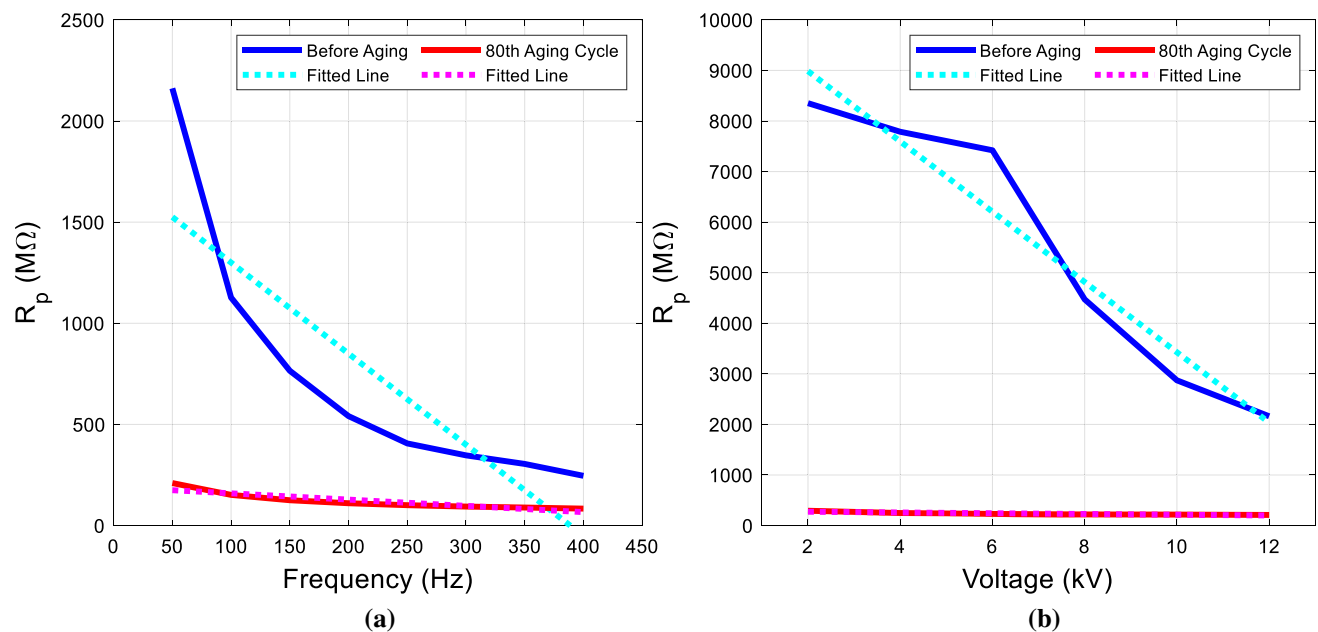


**Fig. 11** Measurements results of  $R_p$ : **a** due to frequency, **b** due to voltage

The gradient of the frequency-dependent  $R_p$  value was determined as  $-4.5026$  before aging. The negative gradient value proved its decreasing behavior. At the end of 80th aging cycle, the gradient on the frequency domain has reached the value  $-0.3096$ . Thus, it was revealed that the aging effect decreased the amount of decrease. When the voltage-dependent  $R_p$  value is examined, it is determined that the gradient is  $-695.035$ . Because of this value is negative, it revealed the decrease in the value of  $R_p$  due to the voltage. At the end of 80th aging cycle, this value reached  $-7.3803$ .

It is seen that the resistance value decreases with increasing frequency, and the current increases with increasing measuring voltage, so the dielectric loss values, which are directly proportional to the square of the current, increase. It has been determined that the dielectric performance is dosed by affecting the cable impedance due to harmonic orders.

## 6 Conclusion

In this study, aging process was performed on 12/20.8 kV XLPE power cable samples with 60 kV overvoltage ( $5 \cdot U_0$ ) in Yıldız Technical University High Voltage Laboratory. Dielectric parameter measurements were performed after each aging cycle. The dielectric parameters ( $P_K$ ,  $\tan\delta$ ,  $C_p$  and  $R$ ) of the aged cable samples were measured. By using OMICRON CPC100/CP-TD1 measuring device, the effects of harmonics with different measurement voltages have been examined. Disruptive effect of harmonics have been revealed by the analyses made by aging cycles.

Evaluation of measurement results can be made from three different perspectives. The first point of view is to examine the effect of aging on the cable according to frequency and voltage. In this case, the conclusion to be drawn from the study is that the effect of overvoltage at the rated voltage and frequency is seen quite clearly. The second point of view is the comparison of measurements made at different frequencies according to the number of aging cycles and the evaluation of according to each other. In this case, it is seen that the 3rd–5th–7th harmonics orders are effective for the  $\tan\delta$  and  $P_K$  value based on measurement results. The third and last point of view is to investigate the negative effect on the cable as a result of the increase in the effective value of the voltage together with the harmonic components. In this study, it is clearly seen that  $P_K$ ,  $\tan\delta$  and  $C_p$  values increase with the voltage value during the measurement of dielectric parameters. However, the rate of increase in the capacity value is considered to be negligible. In this case, the results obtained from this study are stated below as items.

- The negative effect of overvoltage on underground cables has been proven by the change in dielectric parameters depending on aging.
- As a result of  $\tan\delta$  measurements, it was observed that the dielectric quality of the cable insulation material deteriorated due to overvoltage.
- After the 40th aging cycle, the highest decrease in  $\tan\delta$  value occurred in the 5th and 7th harmonic components and this rate was 2.7%. When it comes to the 80th cycle, it is seen that the 3rd order harmonic component causes the highest decrease with 1.5%. As a result, the distortion

occurring at the frequency of 150–250–350 Hz has a more negative effect on the  $\tan\delta$  value.

- The  $P_K$  formed in the cable insulation material increased due to the overvoltage.
- The increase in  $P_K$  at 150 Hz frequency was 94.6% at the end of the first 20 aging. It is revealed that the 3rd (150 Hz) harmonic component produces the highest increase in the data analyzed every 20 cycles comparatively. But, when looking to values of 80th aging cycles, it has been determined that the harmonics of 3–5–7 degrees are factor that most affects the  $P_K$  value.
- The effect of frequency and voltage changes on  $\tan\delta$  and  $P_K$  is quite similar.
- The  $C_p$  value was not affected by the overvoltage aging process.
- The  $C_p$  value was not affected by harmonic components, acting independently of the measurement voltage and frequency.
- The frequency effect increased with increasing voltage value due to harmonic components.
- Effects of harmonic orders should not be ignored in the creation of maintenance and replacement activities about power cables.

The study showed that more attention should be paid to the effects of harmonics in distribution systems containing harmonics of 3–5–7th order. As a result, it is necessary to accept that the dielectric parameters of the equipment in the power system change due to harmonic components and to observe this change closely. In this context, it is emphasized that the insulation quality of the equipment used in power systems should be evaluated by including harmonic components. In this context, increasing effects of harmonic order due to aging should be considered in the evaluation of economic losses in power systems.

**Acknowledgements** Scientific Research Project Coordinator of Yildiz Technical University supported this research study with the project number FDK-2020-3897. The authors would like to thank the Yildiz Technical University for financial support.

## References

1. Uribe FA, Nuño V, Barocio E, Zuniga P, del Puerto-Flores D (2018) Synthesizing electrical signals with harmonic and inter-harmonic components through generalized Fourier series. *Electr Eng* 100(2):557–564. <https://doi.org/10.1007/s00202-017-0525-3>
2. Rashid Z (2021) Calculation of overhead and underground cable parameters at harmonic frequencies. *Electr Eng* 103(1):729–741. <https://doi.org/10.1007/s00202-020-01119-y>
3. Taslak E, Arikan O, Kumru CF, Kalenderli O (2018) Analyses of the insulating characteristics of mineral oil at operating conditions. *Electr Eng* 100(1):321–331. <https://doi.org/10.1007/s00202-016-0501-3>
4. Morgan VT (1998) Effects of frequency, temperature, compression, and air pressure on the dielectric properties of a multilayer stack of dry kraft paper. *IEEE Trans Dielectr Electr Insul* 5(1):125–131. <https://doi.org/10.1109/94.660818>
5. Bahadoorsingh S, Rowland SM (2010) Investigating the impact of harmonics on the breakdown of epoxy resin through electrical tree growth. *IEEE Trans Dielectr Electr Insul* 17(5):1576–1584. <https://doi.org/10.1109/TDEI.2010.5595560>
6. Abderrazzaq MH, Hussin MS, Alhayek K (2013) The effect of high frequency, high voltage supply on the growth of electrical trees on cross linked polyethylene insulation of power cables, In: Proceedings of IEEE international conference of solid dielectric. ICSD, pp. 812–815, doi: <https://doi.org/10.1109/ICSD.2013.6619897>
7. Mittal L, Sarathi R, Sethupathi K (2015) Electrical treeing in XLPE cable insulation at cryogenic temperature under harmonic AC voltages. *Cryogenics (Guildf)* 71:62–67. <https://doi.org/10.1016/j.cryogenics.2015.05.010>
8. Sarathi R, Nandini A, Tanaka T (2012) Understanding electrical treeing phenomena in XLPE cable insulation under harmonic AC voltages adopting UHF technique. *IEEE Trans Dielectr Electr Insul* 19(3):903–909. <https://doi.org/10.1109/TDEI.2012.6215093>
9. Sarathi R, Oza KH, Pavan Kumar CLG, Tanaka T (2015) Electrical treeing in XLPE cable insulation under harmonic AC voltages. *IEEE Trans. Dielectr. Electr. Insul.* 22(6):3177–3185. <https://doi.org/10.1109/TDEI.2015.005022>
10. Birlle M, Leu C (2013) Breakdown of polymer dielectrics at high direct and alternating voltages superimposed by high frequency high voltages, In: Proceedings of IEEE international conference of solid dielectric. ICSD, pp. 656–661, doi: <https://doi.org/10.1109/ICSD.2013.6619851>
11. Chien CH, Bucknall RWG (2007) Analysis of harmonics in subsea power transmission cables used in VSC-HVDC transmission systems operating under steady-state conditions. *IEEE Trans Power Deliv* 22(4):2489–2497. <https://doi.org/10.1109/TPWRD.2007.905277>
12. Fard MA, Farrag ME, Reid A, Al-Naemi F (2019) Electrical treeing in power cable insulation under harmonics superimposed on unfiltered HVDC voltages. *Energies*. <https://doi.org/10.3390/en12163113>
13. Guastavino F, Centurioni L, Dardano A, Torello E (2004) Electrical treeing inception and growth in XLPE in presence of harmonics, In: Proceedings of IEEE international conference of solid dielectric. ICSD, vol. 1, pp. 363–366, doi: <https://doi.org/10.1109/icisd.2004.1350366>
14. Kridsanonont J, Xining L, Yanjie C, Shengchang J (2018) Impact of harmonics on needle-plane partial discharge in oil-paper insulation, In: Proceedings of the IEEE international conference on properties and applications of dielectric material, vol. 2018-May, no. 28, pp. 512–516, doi: <https://doi.org/10.1109/ICPADM.2018.8401041>
15. Li W, Li J, Zhou F, Wang S, Li H, Li S (2012) The effect of frequency on the breakdown of XLPE cable insulation with artificial defects, In: Annual report - conference on electrical insulation and dielectric phenomena, CEIDP, pp. 375–378, doi: <https://doi.org/10.1109/CEIDP.2012.6378798>
16. Sonerud B, Bengtsson T, Blennow J, Gubanski SM (2006) Dielectric response measurements utilizing non-sinusoidal waveforms, In: Annual report - conference on electrical insulation and dielectric phenomena, CEIDP, pp. 43–46, doi: <https://doi.org/10.1109/CEIDP.2006.312058>
17. Megherbi M, Bitam-Megherbi F, Benamrouche N (2009) Experimental approach of dielectric losses measurement in insulating paper under distorted voltage stress. *Electr Power Components Syst* 37(7):798–812. <https://doi.org/10.1080/15325000902762372>
18. Montanari GC, Fabiani D (1999) The effect of non-sinusoidal voltage on intrinsic aging of cable and capacitor insulating materials.

- IEEE Trans Dielectr Electr Insul 6(6):798–802. <https://doi.org/10.1109/94.822018>
19. Patil KD, Gandhare WZ (2011) Effects of harmonics in distribution systems on temperature rise and life of XLPE power cables, In: *2011 international conference on power and energy systems*, doi: <https://doi.org/10.1109/ICPES.2011.6156680>.
  20. Subramaniam A, Sahoo A, Manohar SS, Panda SK (2017) Voltage and current-harmonics induced ageing in electrical insulation. *Proc Int Symp Electr Insul Mater* 1(September):403–406. <https://doi.org/10.23919/iseim.2017.8088770>
  21. Wu J, Jin H, Mor AR, Smit J (2017) The effect of frequency on the dielectric breakdown of insulation materials in HV cable systems. *Proc Int Symp Electr Insul Mater* 1:251–254. <https://doi.org/10.23919/iseim.2017.8088734>
  22. Linde T, Loh JT, Kornhuber S, Backhaus K, Schlegel S, Großmann S (2021) Implications of nonlinear material parameters on the dielectric loss under harmonic distorted voltages. *Energies* 14(3):663. <https://doi.org/10.3390/en14030663>
  23. Florkowska B, Florkowski M, Zydron P (2007) The role of harmonic components on partial discharge mechanism and degradation processes in epoxy resin insulation, In: *2007 international conference on solid dielectrics ICSD*, pp. 560–563, doi: <https://doi.org/10.1109/ICSD.2007.4290875>.
  24. Wong JK, Illias HA, Mokhlis H, Bakar AHA (2014) Investigation of partial discharge severity at XLPE cable without termination, In: *Proceeding - 2014 IEEE international conference on power and energy, PECon 2014*, pp. 13–16, doi: <https://doi.org/10.1109/PECON.2014.7062405>
  25. He D, Wang W, Lu J, Teyssedre G, Laurent C (2016) Space charge characteristics of power cables under AC stress and temperature gradients. *IEEE Trans Dielectr Electr Insul* 23(4):2404–2412. <https://doi.org/10.1109/TDEI.2016.7556519>
  26. He D, Gu J, Wang W, Liu S, Song S, Yi D (2017) Research on mechanical and dielectric properties of XLPE cable under accelerated electrical-thermal aging. *Polym Adv Technol*. <https://doi.org/10.1002/pat.3901>
  27. He D, Meng F, Liu H, Li Q, Wang X (2019) The influence mechanism of semiconductive material on space charge accumulation in HVDC cable accessory. *IEEE Trans Dielectr Electr Insul* 26(5):1479–1486. <https://doi.org/10.1109/TDEI.2019.008077>
  28. BS EN 60071-1:2019 Insulation co-ordination Part 1: Definitions, principles and rules. BSI Standarts Limited, 2018.
  29. *BS EN 60071-2:2018 Insulation co-ordination Part 2: Application guidelines*. BSI Standarts Limited, 2018.
  30. IEEE Guide for Accelerated Aging Tests for Medium-Voltage (5 kV–35 kV) Extruded Electric Power Cables Using Water-Filled Tanks (2008) vol. 2007
  31. HD 605 S2 Electric cables - Additional test methods. (2009)
  32. Sivaraman P, Sharmeela C (2021) Power system harmonics
  33. IEEE Std 519, “IEEE Std 519-2014 (Revision of IEEE Std 519-1992), IEEE recommended practice and requirements for harmonic control in electric power systems, In: IEEE Std 519–2014 (Revision IEEE Std 519–1992), vol. 2014, pp 1–29, 2014, [Online]. Available: <http://ieeexplore.ieee.org/servlet/opac?punumber=6826457>
  34. European Standard (2005) En 50160 voltage characteristics of electricity supplied by public distribution systems, pp 1–20
  35. Arora R, Mosch W (2011) High Voltage and Electrical Insulation Engineering. IEEE Press, New Jersey
  36. CPC 100 User Manual.OMICRON ELECTRONICS CORP. (2007)
  37. Das-Gupta DK, Scarpa PCN (1996) Polarization and dielectric behavior of ac-aged polyethylene. *IEEE Trans Dielectr Electr Insul* 3(3):366–374. <https://doi.org/10.1109/94.506208>

**Publisher's Note** Springer Nature remains neutral with regard to jurisdictional claims in published maps and institutional affiliations.

Springer Nature or its licensor holds exclusive rights to this article under a publishing agreement with the author(s) or other rightsholder(s); author self-archiving of the accepted manuscript version of this article is solely governed by the terms of such publishing agreement and applicable law.